sciendo

B&H Electrical Engineering, Volume 17, Issue 1, 2023:17-25
ISSN:2566-3143, eISSN:2566-3151, DOI: 10.2478/bhee-2023-0003

Original scientific paper

Submitted: February 14, 2023

Accepted: May 5, 2023

COMPARISON OF TWO DIFFERENT BATTERY CHARGING METHODS

Goran Kujundžić[1,2], Drago Bago[1], Alen Bernadić[1]

Abstract: This paper describes charging of battery stack using model predictive control (MPC) algorithm. Temperature model and hybrid electrical model are used in algorithm. The battery stack consists of four serially connected valve-regulated lead-acid (VRLA) batteries. The objective of the optimization is to charge the proposed battery stack without violating the constraints in order to maintain the battery health. Validation of MPC algorithm for battery charging is performed using comparison between closed-loop MPC simulations and obtained characteristics of actual MPC charging. Previously, the conventional constant current constant voltage (CCCV) algorithm was proved as good, taking into account the degradation effects but not considering the speed of the charging. The comparison between charging of proposed battery stack using MPC algorithm and CCCV algorithm is performed and the comparison in charging proves MPC algorithm as better compared to the CCCV algorithm.

Keywords: temperature model, hybrid electrical model, thermal runaway, state and parameter estimation, model predictive control

INTRODUCTION

The life of valve-regulated lead-acid (VRLA) battery is often considered to be a function of materials and design parameters such as grid alloy and thickness, paste composition, plate thickness and positive active-materials. While it is readily acknowledged that charging can also have a significant impact on life, it is remarkable how little standard charging method have varied over the past several decades [1], [2]. Moreover, the quantum shift in technologies in moving from flooded to VRLA batteries has seen only minimal adjustment to the charging algorithms developed in the first 80 years of the past century. The effect of so-called 'oxygen cycle' operative in VRLA cells has deep impact on the chemistry of the charging process.

Typical charging method consists of four fundamental modes as shown in Figure 1 [3].

Charging methods or algorithms for the VRLA battery may be classified as follows: constant voltage (CV) charging method, constant current (CC) charging method, constant current constant voltage (CCCV) charging method, constant current constant voltage constant voltage (CCCVCV) charging method, intermittent charging (IC) method and interrupted charging control (ICC) method [3], [4]. The CV and CCCV charging methods are the traditional approaches to charging while the CCCVCV is a modified version of the CCCV charging method. IC method is an alternative voltage driven charging method while the ICC method incorporates current pulse width control [5], [6], [7].

Authors in [3] have shown the comparison mentioned above charging methods considering the charging time performance and negative influences of aging factors. Aging factors are grid corrosion, sulfation of negative electrode and water loss.

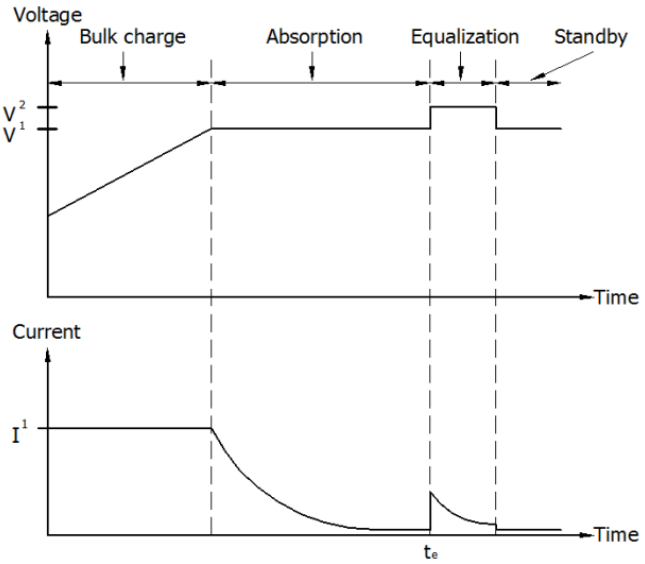


Figure 1: Typical charging method of battery

[1] Faculty of Mechanical Engineering, Computing and Electrical Engineering, University of Mostar, Bosnia and Herzegovina
[2] Correspondence email: goran.kujundzic@fsre.sum.ba
© 2023 Author(s). This is an open access article licensed under the Creative Commons Attribution License 4.0. (http://creativecommons.org/licenses/by/4.0/).

CCCV charging algorithm is the most popular charging regime for VRLA batteries. There are two modes (bulk charge and absorption) in this algorithm, namely the CC charging method followed by the CV method. The battery is charged at a constant current in the CC mode with a bulk charging current until the charging voltage reaches the regulated charging voltage. The battery is then switched to the CV mode where the battery is charged by a tapered current at regulated charging voltage. The regulated charging voltage is set at the recommended float charging voltage given by the battery manufacturer.

Up until about 25 years ago, it has been believed that VRLA batteries could not be fast recharge because there would be irreparable damage to the positive active-material. In addition, in VRLA batteries, it has been felt that this approach would result in excessive levels of grid corrosion and gassing, leading to early, rapid failure. In the early 1990s, Valeriote at Cominco [9] have advanced this technology for, first, flooded lead-acid batteries and, later for thin-plate VRLA batteries. This approach is a variant of standard current-limited CV charging method using additional time-variant resistance in electrical circuit. It has been found that flooded batteries have experienced lower temperature rises due to their high gassing levels and greater volumes of electrolyte, in spite of their higher battery resistances in compared to VRLA batteries. Ohmic factors dominate heat generation at high charging rates up to 40-50% state of charge (SOC), at which point polarization and enthalpic heating become dominant in VRLA batteries. Later work on Hawker Genesis [10], thin-plate, VRLA products demonstrated that simple CV charging with high current limit could be carried out on individual batteries in laboratory tests. To reduce corrosion e and hydrogen generation inside the battery, the lead and thin combination is used for electrode design. Contrary to previous beliefs, for VRLA products, the imposition of aggressive charging algorithms that minimize effects of oxygen cycle and finish the charge relatively quickly can result in superior cycle-life.

In the past 10 years model predictive control is used more for battery charging due to its possibilities of satisfying their constraints (manufacturer upper threshold voltage level, maximum temperature of battery, maximum charging current and maximum SOC). Authors in [8] and [11] have applied MPC for charging of lithium-ion batteries considering these battery constraints. They have shown that model predictive control (MPC) application for charging slightly reduces the lifetime of battery, achieving faster battery charging compared to the charging using conventional algorithms. To predict battery behaviour authors in [8] have used electrical RC model and temperature model identified using neural network. In [11] input-output models for electrical and temperature model have been used. They have been identified from measured responses using least square method.

This paper proposes new charging method of VRLA batteries using MPC approach. The goal is to achieve faster charging of VRLA batteries opposite to using CCCV algorithm. Constraints that must be satisfied are: manufacturer battery voltage, the maximum increase of battery temperature - compared to the ambient temperature, saturation at high SOC, maximum charging current and maximum SOC. Maximum charging current is limited to a lower value of the current C_1 (C_1 – one-hour charging rate), because the charging is carried out on VRLA batteries, which have a higher internal resistance (thicker-plate electrodes), and also to avoid rapid hydrogen/oxygen generation and increased rates of corrosion in the battery cells. This type of batteries is used in telecommunication power systems and Uninterruptible Power Supplies (UPS).

This paper is organized as follows: Section I presents temperature model of VRLA battery and the way of its parameter identification. In Section II hybrid electrical model and its parameter are defined. In addition, Section II defines the constraint due to battery stack saturation at high states of charge. Experimental test system of VRLA 48 V battery stack of nominal capacity 45 Ah Ritar with all elements is shown in Section III. Also, formulation of MPC charging algorithm that uses temperature and hybrid electrical battery model with all constraints is defined. In Section IV MPC charging results of proposed battery stack and comparison with MPC model simulations are shown. MPC charging performance of VRLA battery stack and comparison with CCCV charging performance previously implemented on the same battery stack is presented after validation of MPC charging algorithm using MPC model simulations.

1. TEMPERATURE MODEL OF VRLA BATTERY

The ambient and battery temperatures are very important values during the charging of VRLA battery. These parameters define how long the battery can be charged with without damaging it and reducing its life. The actual value of battery temperature is not known because VRLA batteries are sealed, and it's not possible to insert the thermometer inside them. Authors in [12] have measured battery temperature inside the electrolyte using a thermometer inserted during production of the battery. The temperatures were measured on few places on battery surface. After measuring with various charging currents, it has been presented that all external measured temperatures followed the battery or cell temperature very well.

In this paper ambient temperature and negative terminal temperature of proposed battery stack are measured. Temperature model of battery stack for charging is defined using obtained temperature characteristics.

B&H Electrical Engineering, Volume 17, Issue 1, 2023:17-25
ISSN:2566-3143, eISSN:2566-3151, DOI: 10.2478/bhee-2023-0003

1.1. Temperature model presentation

In order to determine temperature model, VRLA 48 V battery stack, with nominal capacity 45 Ah Ritar is used. It consists of four 12 V batteries connected in series. This battery stack is also used in [14]. Before the test battery stack was not used and only it was charged in order to equalize the charge of each 12 V batteries. Battery monitoring with acquisition card PIC18F2550 is used for measuring of four 12 V battery voltages, battery stack voltage, charging/discharging current, ambient temperature and negative terminal temperature. Simple electric circuit is used for determination of general VRLA battery temperature model expression. This circuit, shown in Figure 2, consists of elements which represent: ambient temperature (T_a), battery temperature (T_{batt}), thermal resistance (R) and thermal capacity (C). The right side of proposed circuit shows: the term $k \cdot I_{batt}^2$ that presents Joule heating caused by the ohmic resistance of the conducting elements including the electrolyte (internal resistance) and the term $k_1 \cdot sgn(I_{batt})$ that presents the reversible heat effect determined by thermodynamic data of the cell reaction. The equation that describes proposed electric circuit is defined as follows:

$$C \cdot \frac{dT_{batt}}{dt} = k \cdot I_{batt}^2 + k_1 \cdot \mathrm{sgn}\left(I_{batt}\right) + \frac{T_a - T_{batt}}{R}. \quad (1)$$

Application of the Euler discretization on expression (1) results with temperature model of VRLA battery as follows:

$$T_{batt}(k+1) = a_1 \cdot T_{batt}(k) + a_2 \cdot T_a(k) + a_3 \cdot I_{batt}^2(k) + a_4 \cdot \mathrm{sgn}\left(I_{batt}(k)\right). \quad (2)$$

where k=60 is sampling time. Coefficients a_1-a_4 in expression (2) are unknown values that need to be calculated. To determine model coefficients, charging/discharging tests of proposed battery stack need to be conducted. Obtained temperature model for charging/discharging should describe behaviour and changes of battery temperature for operating area of charging/discharging current rates, which are used for coefficient determination.

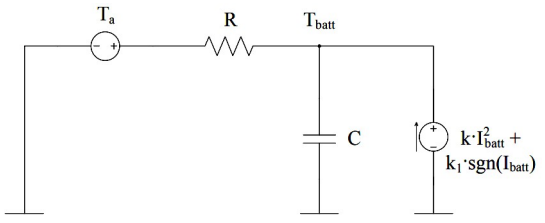


Figure 2: Temperature model of battery

1.2. Coefficient identification of temperature model for battery charging

Coefficients of temperature model for charging are determined using actual test characteristics of both ambient and battery temperatures. Test characteristics were measured during the charging battery stack with various current rates (5 A, 9 A, 14 A and 18 A). Application of the Method of Least Squares on test data, coefficients a_1-a_4 from equation (2) are determined. Obtained temperature model should describe temperature behaviour of the battery stack for each current rate until 18 A. Both ambient and battery temperatures from charging test of battery stack with current 9 A are shown in Figure 3.

Coefficients of temperature model (a_1-a_4) for charging with all current rates are calculated using Method of Least Squares [15] in form:

$$A \cdot x = b, \quad (3)$$

where $A \in \Re^{mxn}$ and $b \in \Re^m$ $(\mathrm{m} > \mathrm{n})$.

Matrix A and b are augmented with all test data and defined by following expressions:

$$A = \left[A;\ \ T_{batt}(k)\ \ T_a(k)\ \ I_{batt}^2(k)\ \ \mathrm{sgn}\left(I_{batt}(k)\right)\right],$$
$$b = \left[b;\ \ T_{batt}(k+1)\right]; k = 60. \quad (4)$$

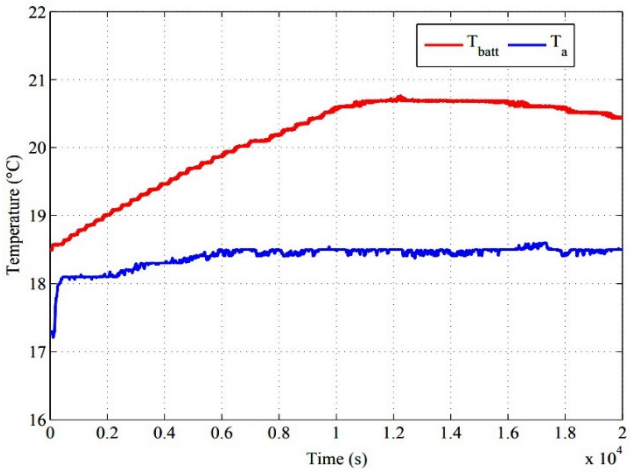


Figure 3: Battery and ambient temperatures (T_{batt}, T_a) - charging with current 9 A

Coefficient vector $x=[a_1\ \ a_2\ \ a_3\ \ a_4]$ are obtained by calculating the equation $x=A\backslash b$.

The final temperature model of VRLA battery stack is obtained using calculated coefficient vector:

$$T_{batt}(k+1) = 0,9958 \cdot T_{batt}(k) + 0,0048 \cdot T_a(k) + 1,0654 \cdot 10^{-4} \cdot I_{batt}^2(k) + 0,0033 \cdot sgn(I_{batt}(k)). \quad (5)$$

In order to validate equivalent temperature model for charging, two comparisons between temperature model and actual charging test measurements are analysed and as shown in Figure 4 and Figure 5. Equivalent battery stack is charged using CCCV charging algorithm with two different charging current rates (9 A and 14 A). The current

charging characteristics are also shown in these figures. As shown, it can be concluded that this temperature model has same trend as these test measurements with both charging current rates. Deviations of temperature model are small for both current rates. Temperature model deviates more from test measurements for charging current rate 14 A than for 9 A. Maximal difference between temperature model and actual battery temperature is about 0,3 ℃. This deviation or model error needs to be taken into account when using this temperature model.

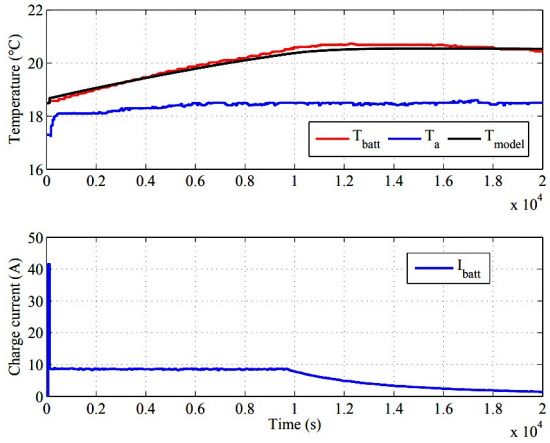


Figure 4: Comparison between experimental results and model simulation – charging with current 9 A

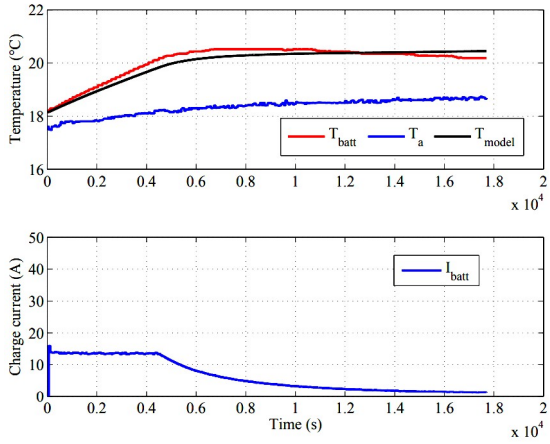


Figure 5: Comparison between experimental results and model simulation – charging with current 14 A

2. HYBRID ELECTRICAL MODEL

Hybrid electrical model of a battery is shown in Figure 6. It consists of two parts (left and right part of electrical circuit). Left part of electrical circuit contains capacitor $C_{capacity}$, self-discharge resistor R_{self} and current-controlled current source I_{batt}, while right part of circuit consists of voltage-controlled voltage source V_{OC} (V_{SOC}), resistors (R_{serial}, R_{fast}, and R_{slow}) and capacitors (C_{fast}, and C_{slow}).

V_{OC} is open-circuit voltage of the battery and V_{SOC} represents the state-of-charge (SOC) of the battery quantitatively. If V_{SOC} is equal to 1 or 0 V, the battery is fully charged (SOC is 100%) or fully discharged (SOC is 0%).

This hybrid electrical model is completely described in [13] and [14]. Also, in this paper are used the same battery stack with experimental setup and method of identification of battery parameters as in previous paper [14]. The obtained values of battery parameters (R_{serial}, R_{fast}, R_{slow}, C_{fast} and C_{slow}) of hybrid electrical model and presented in Appendix.

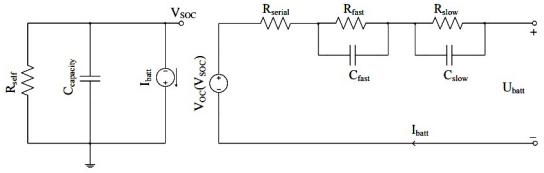


Figure 6: Hybrid electrical model of a battery

2.1. Saturation constraint determination

Figure 7 shows typical safe operating area for a VRLA battery. Thermal and saturation stress limits are not fixed, and they dynamically adjust as the battery's SOC rises during the charging. The charging rate is below the limit defined with blue line (charging rate values are lower than current C_1) in first operating area so the battery would not overheat. Initial charging current value is defined by manufacturer. When the battery reaches saturation area, charging rate is linearly reduced as the battery's SOC rises. In this case, the charging rate is below the limit defined with red line.

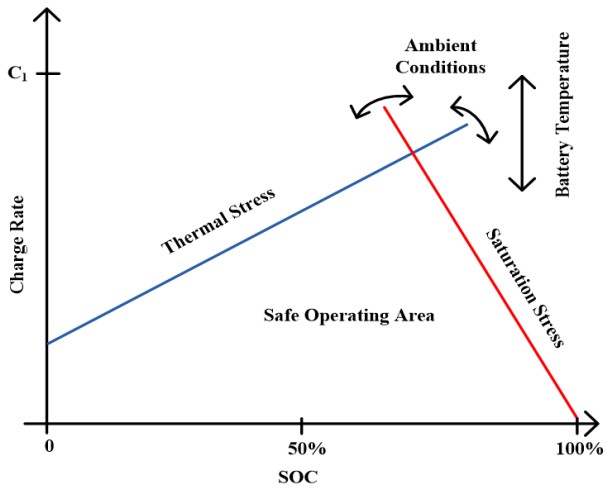


Figure 7: Safe operating area of VRLA battery

The saturation constraint is defined by following expression:

$$I_{batt} \le c \cdot SOC + d, \tag{6}$$

where c and d are coefficients of linear constraint that has to be identified.

In order to define saturation constraint of proposed battery stack, voltage and current measurement data

B&H Electrical Engineering, Volume 17, Issue 1, 2023:17-25
ISSN:2566-3143, eISSN:2566-3151, DOI: 10.2478/bhee-2023-0003

for the charging with current rates (5 A, 9 A, 14 A and 18 A) are used. All previously mentioned tests are conducted in the same ambient temperature to achieve the same SOC point with defined current rate. After that, using saturation point on voltage-time curve, SOC values are identified for each current rate. Coefficients c and d of linear constraint are determined using four obtained SOC points and shown in Appendix.

To make valid comparison between charging using MPC algorithm and CCCV charging algorithm, constant charging current will be used in first operating area while ensuring that the negative terminal temperature of battery stack does not go over allowed constraint.

3. APPLICATION OF MODEL PREDICTIVE CONTROL FOR CHARGING

3.1. Experimental setup

Experimental setup is same as in previous paper [14]. Battery monitoring consists of voltage sensors, two temperature sensors, current transformer and acquisition card type USB PIC18F2550, IO Board, Microchip Technology. DC 48 V charger Delta with controller PSC 3 is used for charging of the battery stack.

3.2. MPC formulation

As described in [14] model predictive control is a control strategy, which at each sampling instant solves a finite horizon optimal control problem over the future behaviour of the system. In this case (battery charging), the objective function of the optimization is to charge the battery as fast as possible without violating the constraints in order to maintain the battery health. The hybrid electrical model of the battery requires estimates the battery SOC, the battery voltage U_{batt} and the voltages V_{fast} (voltage at fast transient RC network) and V_{slow} (voltage at slow transient RC network) These voltages representing the fast and slow dynamics of the battery. In addition, a temperature model of the battery is used in order to avoid unnecessary overheating of the battery during the charging of the battery stack.

The only measurable variables in the system are the battery voltage U_{batt} and the battery temperature T_{batt} while the control input is the battery current I_{batt} (k). In order to synthesise a model predictive controller a state-space model of the battery is converted to discrete-time transfer functions:

$$G_1(z)=\frac{U_{batt}(z)}{I_{batt}(z)}, \tag{7}$$

$$G_2(z)=\frac{V_{OC}(z)}{I_{batt}(z)}. \tag{8}$$

Based on the corresponding transfer functions, only the previous values of the battery voltage and the battery current are needed to estimate the future behaviour of the corresponding battery voltages U_{batt} and V_{OC}. The state of charge SOC can be directly calculated from the voltage V_{OC} according to the following relations:

$$V_{OC}=a\cdot V_{SOC}+b;\quad \mathrm{SOC}=100\cdot \mathrm{V_{SOC}}, \tag{9}$$

where a and b are parameters which define V_{OC}.

The non-linear discrete-time temperature model (5) can be directly used for model predictive control purposes.

The corresponding model used in a model predictive control algorithm is denoted for brevity as:

$$\begin{aligned} x(k+1)&=f\left(x(k),x(k-1),...,I_{batt}(k),I_{batt}(k-1),.\right)\\ y(k)&=h\left(x(k),x(k-1),...\right), \end{aligned} \tag{10}$$

where vector $x(k)$ represents a vector of measurable values $[U_{batt}(k),\ T_{batt}(k)]$ while the vector $y(k)$ represents the vector $[U_{batt}(k),\ V_{OC}(k),\ T_{batt}(k)]$.

The objective function is chosen to maximize the state of charge over the prediction horizon N:

$$\mathrm{J}(k)=\sum_{j=0}^{N}\left(1-V_{SOC}(k+j)\right). \tag{11}$$

The current is constrained to only allow the charging with the admissible charging current:

$$0\geq I_{batt}(k+j)\geq -I_{batt\max},\ j=1,...,N, \tag{12}$$

where the minus sign denotes the charging of the battery.

The battery temperature rise above the ambient temperature $T_a(k)$ is constrained below the maximum allowed value $\Delta T_{battmax}$, as follows:

$$T_{batt}(k+j)\leq \Delta T_{batt\max}+T_a(k+j),\ j=1,...,N, \tag{13}$$

where the ambient temperature is assumed to be constant over the prediction horizon. The battery voltage is constrained below the maximum allowed battery voltage:

$$U_{batt}(k+j)\leq U_{batt\max},\ j=1,...,N. \tag{14}$$

In addition, the model predictive control algorithm exploits the knowledge about the line which determines the maximum allowed state of charge (saturation constraint) obtained by charging the battery with a constant current:

$$I_{batt}(k)\geq c\cdot SOC+d. \tag{15}$$

All the corresponding constraints can be written as set-membership constraints:

$$y(k+j) \in Y, j = 1,...,N, \quad (16)$$

$$u(k+j) \in U, j = 1,...,N. \quad (17)$$

The corresponding model predictive control algorithm can be written as follows:

$$\begin{aligned} &\min_{I_{batt}(k)} J(y(k)) \\ &s.t. x(k+j+1) = \\ &f(x(k+j), x(k+j-1),..., \mathrm{I}_{\mathrm{batt}}(k+j), I_{batt}(k+j-1),...), \\ &j = 1,...,N, \\ &y(k+j) = h(x(k+j), x(k+j-1),...), j = 1,...,N-1, \\ &y(k+j) \in Y, j = 1,...,N, \\ &u(k+j) \in U, j = 1,...,N. \end{aligned} \quad (18)$$

The corresponding optimization problem is non-linear in its nature due to the non-linear temperature model of the battery. In the sequel the simulation and experimental results are presented.

4. EXPERIMENTAL AND SIMULATION RESULTS

Model predictive control algorithm (18) is implemented in experimental system in order to initiate charging the proposed battery stack. All identified values of the parameters shown in Appendix are applied in the algorithm. Charging current of MPC constraint is adjusted to the maximum allowed value $I_{battmax}$=-17.2 A (minus sign denotes the charging of the battery). Battery voltage is limited to upper voltage limit $U_{battmax}$=54.80 V defined by manufacturers. Maximum permitted value of battery temperature increases compared to the ambient temperature is $\Delta T_{battmax}$= 7 °C. This temperature rise is selected so that the battery is safe from the thermal runaway which occurs when the battery temperature increases 10 °C compared to the ambient temperature [16]. Maximum SOC value is adjusted to 100%, and maximum open-circuit voltage to value V_{OCmax}=51.90 V.

4.1. Comparison of the model predictive control experimental and simulation results

Charging of the proposed battery stack was initiated after defining all parameters and constraint values of MPC algorithm. To validate all obtained characteristics of MPC charging which lasted 135 minutes, comparison between these characteristics and closed-loop simulations using the same MPC algorithm is given. Figures 8 - 11 shows obtained comparisons for battery voltage U_{batt}, charging current I_{batt}, battery temperature T_{batt}, and battery SOC.

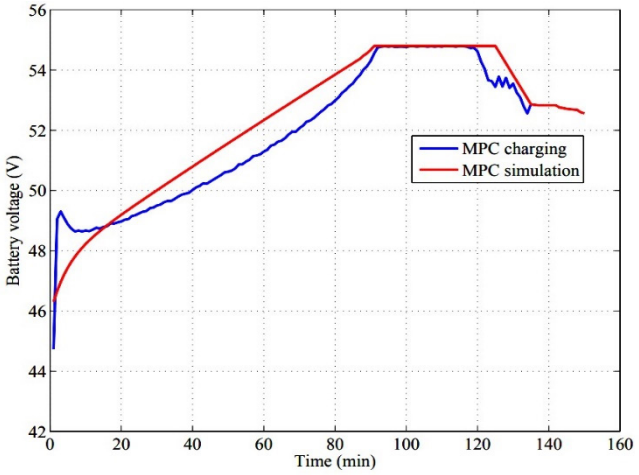


Figure 8: Comparison for battery voltage - MPC charging and simulation

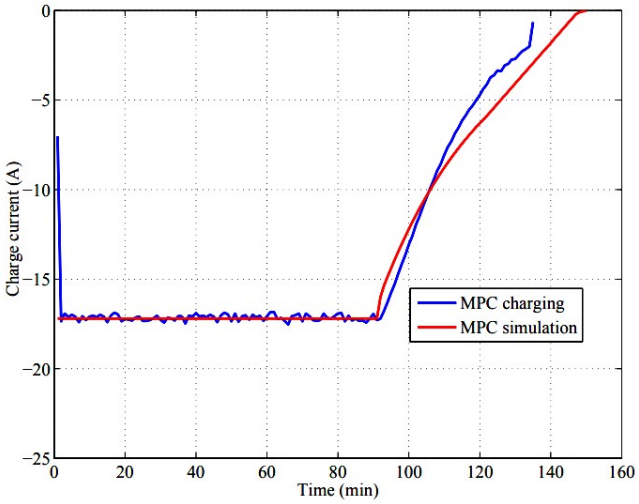


Figure 9: Comparison for charging current - MPC charging and simulation

It took 127 minutes for simulations using MPC algorithm to fully charged battery state which is 8 minutes faster compared to the actual charging. All simulation characteristics describe well the trend of actual charging characteristic behaviour using MPC algorithm. This shows that the MPC algorithm is correct and the difference between experimental and simulation charging is as much as the hybrid electric model deviates from the actual behaviour of the battery. The difference between actual charging and simulation is a consequence of electrical model error which is under 5%. The discrepancy between the hybrid electrical model and the experimental setup is completely described in [13] and [14].

The actual battery temperature during the charging shows deviation compared to the simulation characteristic in Figure 10 which is also a consequence of deviation of temperature model.

B&H Electrical Engineering, Volume 17, Issue 1, 2023:17-25
ISSN:2566-3143, eISSN:2566-3151, DOI: 10.2478/bhee-2023-0003

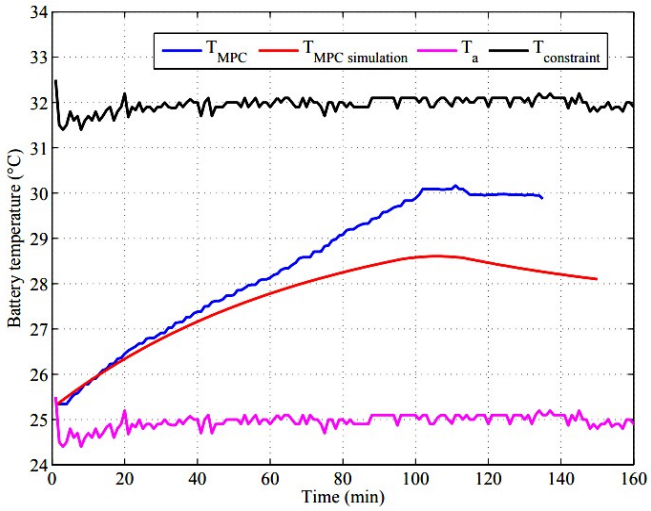


Figure 10: Comparison for battery temperature - MPC charging and simulation

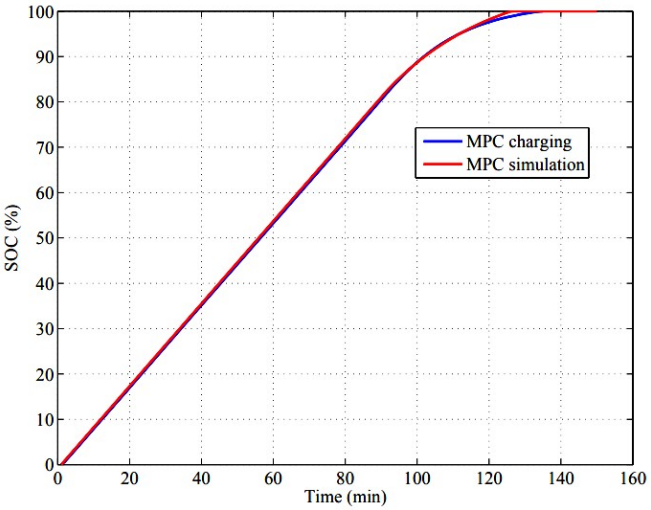


Figure 11: Comparison for battery SOC - MPC charging and simulation

4.2. Comparison of charging algorithms

The conventional CCCV algorithm of battery charging was proved satisfied taking into account the degradation effects but not considering the speed of the charging [3]. In this work it will be tried to get better performance of charging using MPC algorithm with the same constraints of battery. After validation of charging using MPC algorithm, comparison between charging of proposed battery stack using MPC algorithm and CCCV algorithm is performed.

Charging of proposed battery stack is initiated using CCCV algorithm with charging current adjusted to maximum allowed value $I_{battmax}$=-17.2 A, while the battery voltage is limited to upper voltage limit $U_{battmax}$=54.80 V, same as well as for charging using MPC algorithm. All obtained characteristics for battery voltage U_{batt}, charging current I_{batt}, battery temperature T_{batt}, and battery SOC are shown in Figures 12 - 15 to compare performance of CCCV algorithm, on these figures charging characteristics of MPC algorithm are also given.

It can be seen in Figure 12 that battery voltage of CCCV charging reached upper voltage limit in 86 minutes, which is just 6 minutes earlier than using MPC algorithm. On the other hand, charging current (Figure 13) of MPC algorithm retains constant value 6 minutes longer, which results in faster charging of proposed battery stack. It can be noticed that there is a rise of charging current at the beginning of charging using CCCV algorithm, leading to slight increase of battery voltage compared to voltage using MPC algorithm.

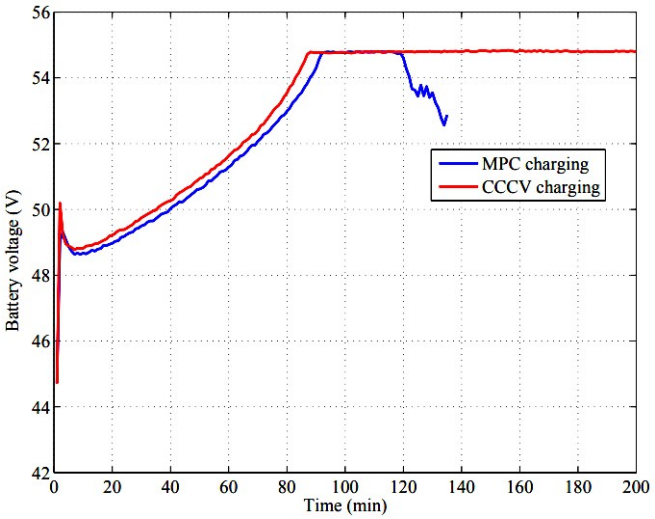


Figure 12: Comparison for battery voltage - MPC charging and CCCV charging

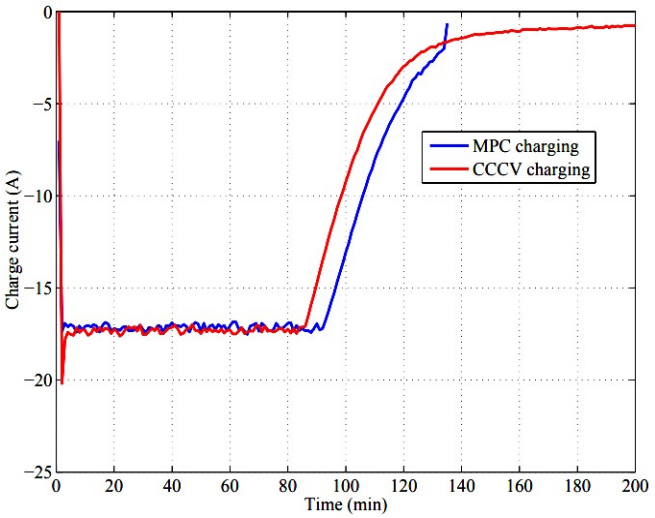


Figure 13: Comparison for charging current - MPC charging and CCCV charging

Battery temperature of both types of charging has similar trend of behaviour and the differences in values between them are small, as shown in Figure 14. Also, in the same figure, the ambient temperature and temperature of constraint are given. It can be seen that the temperatures of both types

of charging are below the constrained temperature, which confirms that degradation effects in proposed battery stack due to temperature rise are small and have slight impact on the reduction of its lifetime. One can see in Figure 15 that both algorithms approximately similarly charge the proposed battery stack until 83% of *SOC*. After this *SOC* point, there is a big difference in charging; MPC algorithm charged the battery stack in 37 minutes at 100% *SOC*, while CCCV algorithm did not reach remaining 17% *SOC* even in 200 minutes of charging.

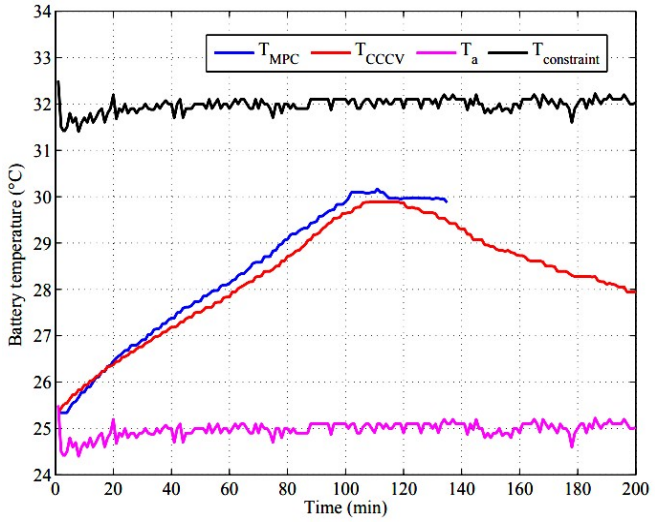


Figure 14: Comparison for battery temperature - MPC charging and CCCV charging

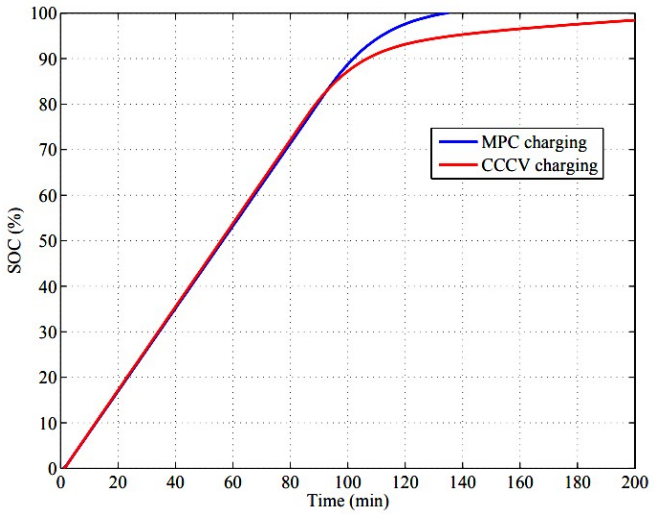


Figure 15: Comparison for battery *SOC* - MPC charging and CCCV charging

Preformed comparison leads to conclusion that the charging of VRLA battery stack using MPC algorithm is faster and has slight impact on the reduction of its lifetime.

5. CONCLUSION

Inadequate control of VRLA battery charging may cause significant damage and degradation effects in batteries, ultimately resulting in the reduction of battery life. The imposition of well-designed charging algorithms that minimize the effects of the internal oxygen cycle and finish the charge relatively quickly can result in superior cycle-life. There is a small number of standard charging methods that have been used over the past several decades. Recently CCCV charging method has been good when taking into account the effects due to the temperature increase of the battery but not considering the speed of the charging. Charging of lithium-ion batteries using MPC algorithm, satisfying all battery constraints, has been more applied recently.

A new charging method of VRLA batteries using MPC algorithm is described in this paper. Hybrid electrical model and temperature model are used in the algorithm for prediction of future states. The goal was to achieve faster charging of VRLA batteries opposite to using CCCV algorithm. The constraints in MPC algorithm were: manufacturer upper threshold voltage level, the maximum battery temperature increase - compared to the ambient temperature, saturation at high *SOC*, maximum charging current and maximum *SOC*. After validation of MPC algorithm for battery charging using closed-loop MPC simulations, comparison between battery charging using MPC algorithm and CCCV algorithm was carried out. Application of MPC algorithm for VRLA battery charging was found faster compared to the charging using CCCV algorithm.

In the further research proposed charging method using MPC algorithm can be applied for fast charging of VRLA batteries with low internal resistance, which are used in electric vehicles. In addition, this algorithm can be used for charging of VRLA batteries in the microgrid environment in order to get their optimal exploitation.

APPENDIX

In this section we give numerical values of all parameters specified in Section I and Section II.

1. Temperature model:
a_1=0.9958; a_2=0.0048; a_3=1.0654 ·10^{-4}; a_4=0.0033.

2. Hybrid electrical model (0–20% SOC):
R_{serial}=0.1395 Ω; R_{fast}=0.0806 Ω; R_{slow}=0.0465 Ω;
C_{fast}=3400 F; C_{slow}=89145 F; $C_{capacity}$=45 Ah;
R_{self}=42.6 $k\Omega$; a =7.90; b =44.

3. Hybrid electrical model (20–80% *SOC*):
R_{serial}=0.1237 Ω; R_{fast}= 0.0787 Ω; R_{slow}= 0.0407 Ω;
C_{fast}= 3360 F; C_{slow}= 88450 F; $C_{capacity}$=45 Ah;
R_{self}= 42.6 $k\Omega$; a = 7.90; b = 44.

4. Hybrid electrical model (80–100% *SOC*):
R_{serial}=0.1724 Ω; R_{fast}= 0.0953 Ω; R_{slow}= 0.0642 Ω;
C_{fast}= 3420 F; C_{slow}= 89100 F; $C_{capacity}$=45 Ah;
R_{self}= 42.6 $k\Omega$; a = 7.90; b = 44.

5. Saturation constraint:
c = 0.9958; d = 0.0048.

B&H Electrical Engineering, Volume 17, Issue 1, 2023:17-25
ISSN:2566-3143, eISSN:2566-3151, DOI: 10.2478/bhee-2023-0003

REFERENCES

[1] T. B. Reddy and D. Linden, Eds., "Linden's Handbook of Batteries," 4th ed. McGraw-Hill Professional, 2011.
[2] P. M. Hunter, "VRLA battery float charge: Analysis and optimisation," Ph.D. dissertation, Univ. Canterbury, Christchurch, New Zealand, 2003.
[3] Y. S. Wong, W. G. Hurley and W. H. Wolfle, "Charge regime for valve-regulated lead-acid batteries: Performance overview inclusive of temperature compensation," J. Power Sources, 183 (2008) 783–791.
[4] E. Rossinot, C. Lefrou, F. Dalard and J. P. Cun, "Batteries in standby applications: comparison of alternate mode versus floating," J. Power Sources, 101 (2001) 27–34.
[5] M. Bhatt, W. G. Hurley and W. H. Wolfle, "A New Approach To Intermittent Charging of Valve-Regulated Lead-Acid Batteries in Standby Applications," Industrial Electronics Magazine, IEEE Transaction on, vol. 52, pp. 1337–1342, 2005.
[6] P. Waltari, T. Suntio, A. Tenno and R. Tenno, "The Effects of Intermittent Charging on VRLA Battery Life Expectancy in Telecom Application," Proceedings of 24th International Telecommunications Energy Conference (INTELEC), pp. 121–127, 2002.
[7] Y. S. Wong, W. G. Hurley and W. H. Wolfle, "Temperature Compensation Algorithm for Interrupted Charge Control Regime for a VRLA Battery in Standby Applications," Proceedings of IEEE Applied Power Electronics Conference and Exposition (APEC 2008), pp. 1278–1283, 2008.
[8] J. Yan, G. Xu, H. Qian and Y. Hu, "Battery Fast Charging Strategy Based on Model Predictive Control," 72nd Vehicular Technology Conference, 2010 IEEE, pp. 1–8, 2010.
[9] E. M. Valeriote, J. Nor and V. A. Ettel, Proceedings of the 5th International Lead-Acid Battery Seminar, International Lead Zinc Research Organization (ILZRO), Inc., Research Triangle Park, NC, USA, pp. 93–122, 1991.
[10] F. A. Fleming, P. Shumard and B. Dickinson, "Rapid recharge capability of valve-regulated lead-acid batteries for electric vehicle and hybrid electric vehicle applications," J. Power Sources, 78 (1999) 237–243.
[11] M. Torchio, N. A. Wolff, D. M. Raimondo, L. Magni, U. Krewer, R. B. Gopaluni, J. A. Paulson and R. D. Braats, "Real-Time Model Predictive Control for the Optimal Charging of a Lithium-ion Battery," Proceedings of American Control Conference (ACC), 2015, 4536-4541, 2015.
[12] F. J. Vaccaro, J. Rhoades and B. Le, "VRLA battery temperature concerns other than just thermal runway. I. Practical considerations," Proceedings of 18th International Telecommunications Energy Conference (INTELEC), pp. 39–44, 1996.
[13] G. Kujundzic, M. Vasak, J. Matusko: Estimation of VRLA Battery States and Parameters using Sigma-point Kalman Filter, 2015 International Conference on Electrical Drives and Power Electronics (EDPE) The High Tatras, 21-23 Sept. 2015.
[14] G. Kujundzic, S. Iles, J. Matusko and M. Vasak, "Optimal charging of valve-regulated lead-acid batteries based on model predictive control," Applied Energy, Elsevier, vol. 187(C) , pages 189-202, 2017.
[15] E. K. P. Chong and S. H. Zak, "An Introduction to Optimization," 2th ed. A Wiley-Interscience Publication, John Wiley&Sons Inc., pp. 187–217, 2001.
[16] E. Boisvert, "Using Float Charging Current Measurement to Prevent Thermal Runaway on VRLA Batteries," 23rd International Telecommunication Energy Conference, Edinburgh INTELEC 2001, pp. 126–131, 2001.

BIOGRAPHY

Goran Kujundžić received the B.S. and Ph.D. degree from University of Zagreb, Croatia in 2000 and 2017 respectively. He worked as a designer and project manager at the Distribution Department of Elektroprivreda HZ HB power utility (2000-2006) and after at Power Department of JP Hrvatske Telekomunikacije Mostar. His research interests include energy storage systems and management of microgrids that are based on renewable sources.

Drago Bago graduated and completed postgraduate PhD studies from the Faculty of Electrical Engineering and Computing, University of Zagreb. Since 2000 he has been employed at JP Elektroprivreda Hrvatske zajednice Herceg Bosne d.d. Mostar in the Distribution Power Division and the Development Division. Now, he is a member of the Board and the Executive Director for Development in JP Elektroprivreda Hrvatske zajednice Herceg Bosne d.d. Mostar. He is an author and a co-author of several scientific and professional papers in the field of overvoltage protection for medium voltage lines, the correlation of events data from the power system and data from the system of professional organization IEEE.

Alen Bernadić was born in Mostar, Bosnia and Herzegovina in 1971. Employed at Electricity Transmission Company of BiH, as Head of department for planning and engineering of operational area Mostar. He is an assistant professor at the Mostar University, Faculty of Mechanical Engineering, Computer Science and Electrical Engineering Faculty (FSRE). He is also an Associate at the University of Split, Faculty of Electrical Engineering, Mechanical Engineering and Naval Architecture (FESB). He has published more than 25 scientific papers in international journals and at international conferences. In the latest research his special interest is AI methods in the power system.